Inter-annual variability of nutrient distribution in the Eastern Tropical North Pacific oxygen deficient zone

Anna C. Bakker

Ocean Sciences Building
1492 NE Boat Street
Seattle, WA 98105

annacb@uw.edu

28 May 2017

ABSTRACT
In Oxygen Deficient Zones (ODZs) in the ocean, anaerobic respiratory processes remove fixed nitrogen from the marine system as nitrogen gas. The expansion of ODZs over time in response to accelerated anthropogenic climate change is of concern, so understanding their unique chemistry is critical. The Eastern Tropical North Pacific (ETNP) is home to the world's largest naturally occurring ODZ, and has been sampled by seven oceanographic transects from 1965 to early 2017. The equatorial Pacific is also subject to El Niño and La Niña phenomena, making the ETNP a physically, chemically, and biologically important system to study. This project's purpose is to use nutrient data from research cruises dating back to 1965 to examine changes in the vertical extent of the ODZ and in nutrient distributions in the ETNP over both short and long timescales. The most recent addition of data to a long-term study was collected on the *R/V Sikuliaq* from December 30th, 2016 to January 15th, 2017. Temporal variability between ODZ vertical extent, nutrient distribution patterns, and El Niño/La Niña were analyzed. The ODZ has increased in thickness by 300 m since 1965. Each year, the nitrite maximum appeared to be permanently bound by the oxycline, while varying in latitudinal extent throughout the years. Current datasets lack the statistical power to determine whether or not ENSO state is driving an increase in the ODZ vertical extent or nutrient distributions, though the observations from this study indicate notable inter-annual variability therein.

INTRODUCTION

This study examines ODZs, a particularly unique marine environment characterized by extremely low oxygen (O_2) concentrations, defined here as < 10 μmol/kg O_2. Anoxia in the ocean is a result of biological, physical, chemical, and geographical processes acting together. Natural ODZs form as a result of weak oceanic ventilation and from continuous respiratory processes that consume O_2 (Fiedler and Talley, 2006; Karstensen et al., 2008; Sarmiento et al. 1988). One of the attributes of an ODZ is that it is occupied by microbial marine species that extract nitrogen (N) instead of O_2 from the water column for anaerobic respiration (Liu et al., 2014). Anaerobic microbes remove bioavailable N, in turn regulating oceanic productivity since N is needed for biomass production (Penn et al., 2016, Tsementzi et al., 2016). In oxic oceans, N_2 gas diffuses into the seawater and is converted to N by nitrogen-fixing bacteria; in anoxic oceans, anaerobic microbes then fix N back to N_2 gas, which results in a loss of a vital nutrient needed by all life (Brunner et al., 2013).

In addition to being chemically and biologically unique, the ETNP is also susceptible to globally important physical processes. The El Niño-Southern Oscillation (ENSO) was described by Cane (2005) as the positive-feedback loop of sea surface temperatures responding to "seesawing" sea level pressures over the equatorial Pacific. Anomalous temperatures and pressures associated with El Niño and La Niña results in compounded effects on the ocean. Both El Niño or La Niña can influence oxygen deficiency because of the important oceanic processes associated with them. When the easterly trade winds over the equatorial Pacific fail, less water is upwelled in the ETNP (El Niño). Less upwelling causes thermal stratification, and less ventilation of the surface waters. Conversely, when easterly trade winds are strong, more upwelling results in more nutrients being delivered to the surface waters (La Niña). This addition of nutrients drives biological productivity, ultimately consuming O_2.

Nutrients indicative of anaerobic microbial processes, nitrite (NO_2^-), nitrate (NO_3^-), and ammonium (NH_4^+), can be used to infer rates of N cycling in ODZ environments (Horak et al. 2016). The five nutrients measured during SKQ 2016-17 were the same five that were measured on the past six cruises to the ETNP so that comparative analysis could be carried out. In addition to NO_2^-, NO_3^-, and NH_4^+, O_2, temperature, salinity, silicate (SiO_4^{2-}) and phosphate (PO_4^{3-}) were also measured from seawater samples collected on the 2016-2017 *R/V Sikuliaq* (SKQ) research cruise. It was hypothesized that nutrient distributions and ODZ vertical thickness will reflect ENSO state. This study also investigated whether nutrient distributions varied on daily or annual timescales.

METHODS

Data from SKQ 2016-17 provided an addition to an ongoing analysis of the ODZ in the ETNP. Measurements were collected on a vertical transect from 22˚ N, -109˚ W to 16˚ N, -106˚ W and in two time-series stations around 20˚ N, -106˚ W (P1) and 16˚ N, -107˚ W (P2, Figure 1). Sensors on a CTD measured salinity, [O_2], temperature, and fluorescence. Seawater samples were collected at depths above, throughout, and below the ODZ with 12 L Niskin bottles. Seawater from the Niskin bottles were triple rinsed and syringe filtered through a 0.22 μmol filter unit and stored in triple rinsed scintillation vials at 4 ˚C. Each vial was split with one aliquot tested aboard and the other stored at -20 ˚C and then processed within 2 months at a core

nutrient facility at the University of Washington. $[NO_2^-]$, $[NO_3^-]$, $[NH_4^+]$, $[SiO_4^{2-}]$, and $[PO_4^{3-}]$ were measured as described in Strickland and Parsons (1972). These measurements were used for all comparative analyses.

Additionally, $[NO_2^-]$ measurements were taken on board from Station P2 to allow a time-series study to be created. $[NO_2^-]$ was measured using the azo dye method originally pioneered by Strickland and Parsons (1972) and updated in the Bermuda Atlantic Time Series Methods Manual by Knap et al. (1997). Each 10 mL seawater sample was briefly incubated with a 0.4 mL dye solution containing 0.2 mL of 1 g N-(1-Naphthyl)-ethylenediamine (NED)/1 L miliQ water with 10% HCl and 0.2 mL of 1 g sulfanilamide/10 mL miliQ water. After allowing the sulfanilamide and NED bind to NO_2^-, a spectrophotometer was used to measure the extinction of the dye at 543 nm to find $[NO_2^-]$ in $\mu mol \cdot L^{-1}$. Spectrophotometer wavelengths were compared to a standard curve to calculate seawater NO_2^- concentration. These measurements were used to compare how $[NO_2^-]$ varies daily versus inter-annually.

Station P2 was located at 16.3˚ N, -107 ˚ W. NO_2^- concentrations at 16.3˚ N was chosen to do a comparative analysis between daily and annual fluctuation. SKQ 2016-17 collected seawater samples from Station P2 for five consecutive days in January 2017. These measurements to analyze daily fluctuation were found using the azo dye method mentions above. NO_2^- concentrations at the exact latitude of 16.3˚N from each cruise year were calculated through linear interpolation.

Codispoti and Richards (1976) published data from the 1972 cruise (TGT66); Taft and Johnson (1994) published data from the 1994 cruise (WOCE P18N); Bullister and Johnson (2008) published data from the 2007 cruise (Clivar); undergraduate students from the University of Washington's School of Oceanography published data from the 2012 cruise (TN278). Horak et al. (2016) has summarized all of the four cruise data. Dr. Horak has also provided data collected from research cruise TGT001 in 1965 and TGT37 in 1969 to aid this study. Nutrient concentrations from all seven cruises were used to evaluate correlation between ENSO events and nutrient distribution in the ODZ.

All data analysis was done in R Studio. Linear interpolation between depth and latitude was calculated to make high-resolution heat maps of each nutrient distribution. Nutrient concentrations (NO_2^-, NO_3^-, NH_4^+, PO_4^{3-}, and SiO_4^{2-}) were plotted against latitude to compare how their spatial distributions have changed over the past 50 years. Measurements collected from coordinates unique to one cruise were taken out to strengthen the comparative analysis between cruises.

The Oceanic Niño Index (ONI) was used to examine ENSO because it represents sea surface temperature in the Niño-3.4 region, which is in the east-central equatorial Pacific from 5˚ S to 5˚ N, 170˚W to 120˚W. The actual ONI value during the month(s) of each cruise was thought to not to be representative of ENSO state. Instead, a 4-month average of ONI values leading up to the cruise was chosen for all analysis (Appendix C).

Further analysis was conducted to find correlations between ENSO state, the ODZ, and nutrient distributions. To run correlation tests, each cruise year received a quantitative value for each of

the following: ONI value, ODZ thickness, ODZ top boundary depth, and depth at which each nutrient reached a specific concentration. Each ONI value was calculated by averaging the 4 ONI values of the 4 months leading up to each respective cruise; these values were already standardized. Each ODZ thickness value was calculated by averaging the vertical extent of the ODZ in meters from each cruise transect; then these values were standardized to a mean. Each ODZ top boundary value was calculated by averaging the depth of the top boundary of the ODZ in meters from each cruise transect; then these values were standardized to a mean. The values for the nutrient analyses were calculated by finding the average depth in meters from each cruise transect that NO_2^-, NO_3^-, PO_4^{3-}, and SiO_4^{2-} reached 0.3 µmol/kg, 15 µmol/kg, 25 µmol/kg, and 2.5 µmol/kg respectively; then these values were standardized to a mean. Correlation tests were run on these standardized values, and p-values were calculated from the correlation tests.

RESULTS

Transects between 14˚ N to 22.5 ˚N from cruises TGT001 1965, TGT37 1969, TGT66 1972, P18N 1994, Clivar 2007, TN278 2012, and SKQ 2016 span over similar ETNP regions, which make them suitable for cross comparison (Figure 1). Some coordinates from TN278 2012 and SQK 2016 were removed because samples were collected outside of the 14˚ N to 22.5˚ N area chosen for comparative analysis. NO_2^- measurements were not collected on cruises TGT001 and TGT37. NH_4^+ measurements were not collected on cruises TGT001, TGT37, TGT66, P18N, and Clivar.

Nutrient concentrations (NO_2^-, NO_3^-, NH_4^+, PO_4^{3-}, and SiO_4^{2-}) showed regular distribution patterns with respect to depth and latitude, but also varied interannually (Figure 1, Appendix A). The NO_2^- maxima appear to vary in depth with respect to the shoaling and deepening top boundary of the ODZ (Figure 1). A region of high [NO_2^-] is particularly found right below the oxycline, but above 400 m.

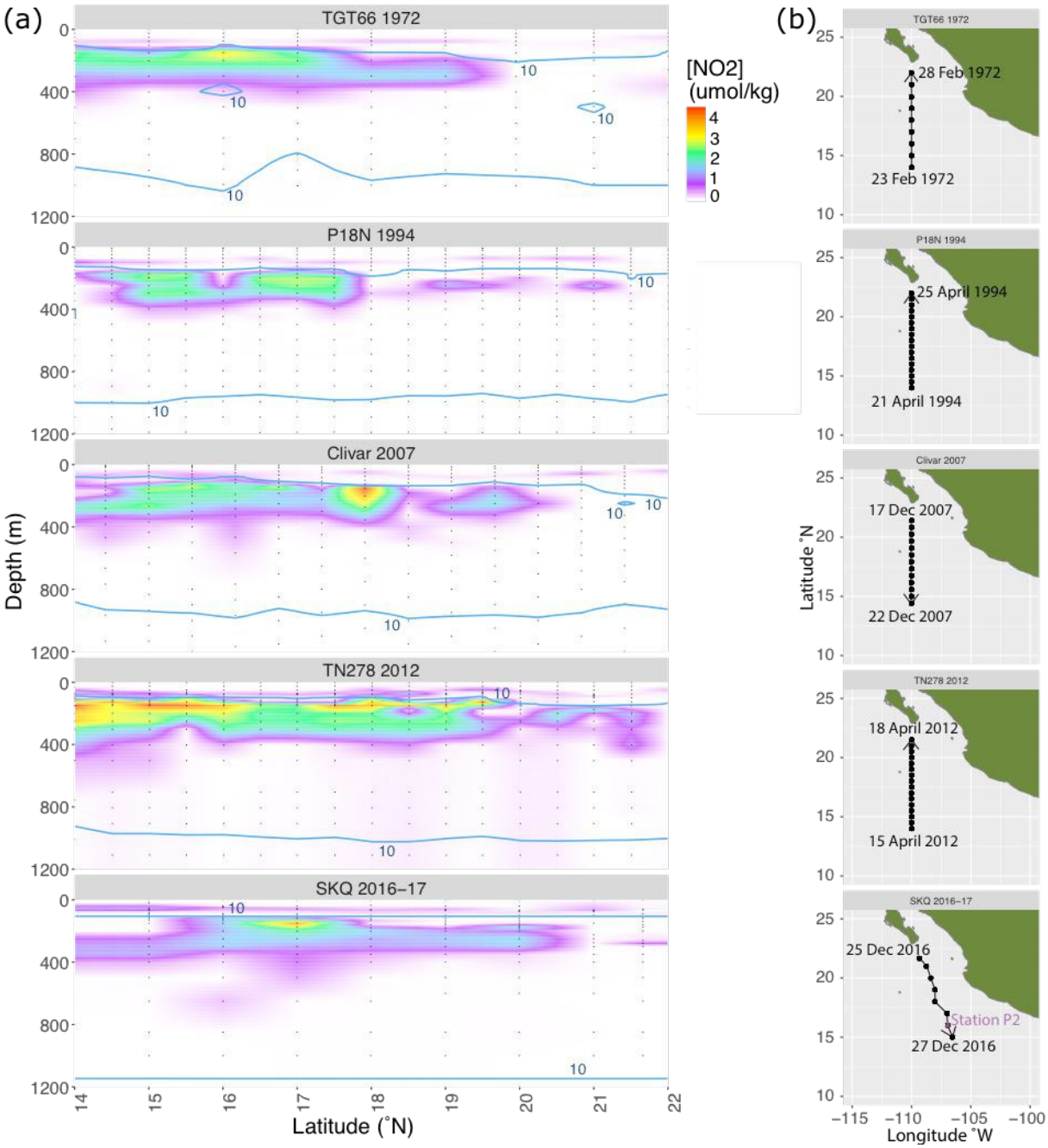

Figure 1 (a) [NO_2^-] as a heat map from 14˚ N to 22.5˚ N. Five out of seven cruises (TGT66, P18N, Clivar, TN278, SKQ) collected NO_2^- data. Vertical dots show where seawater was collected and [NO_2^-] was measured. Spaces between CTD casts are linearly interpolated by depth and latitude. Oxygen contour lines are plotted at 10 µmol/kg. **(b)** Cruise transects off the coast of Baja California and Mexico. Station P2 from SKQ 2016-17 is labeled (purple) to denote the second time-series station (Figure 2).

NO_3^- concentrations increase from 0 to 10 µmol/kg from the surface to the oxycline, but rise up to about 40 µmol/kg at 1,000 m (Appendix Aa). When overlapped with the heat map for NO_2^- concentrations, there is a region in which NO_3^- concentrations drop in half to 20 µmol/kg NO_3^-. PO_4^{3-} concentrations are undetectable in the surface ocean above the oxycline (Appendix Ab). Right before the oxycline, [PO_4^{3-}] rises up to 2 µmol/kg and then is concentrated at 2.5 to 3

µmol/kg throughout the rest of the water column. [SiO_4^{2-}] is below 25 µmol/kg above the oxycline and gradually rises up to around 100 µmol/kg at 1,000 m (Appendix Ac). NH_4^+ concentrations are < 0.5 µmol/kg all throughout the ODZ (Appendix Ad).

[NO_2^-] fluctuated from cruise year to cruise year. [NO_2^-] was high from 14˚ N to 18˚ N during the TN278 2012 cruise and high at 18˚ N during the Clivar 2007 cruise (Figure 1). However, these high values seem to be a function of day-to-day variation instead of year-to-year; NO_2^- appears to show stochastic inter-annual variability in its latitudinal extent (Figure 2). [NO_2^-] was high on the first day but dropped down to near 0 µmol/kg by the fifth day.

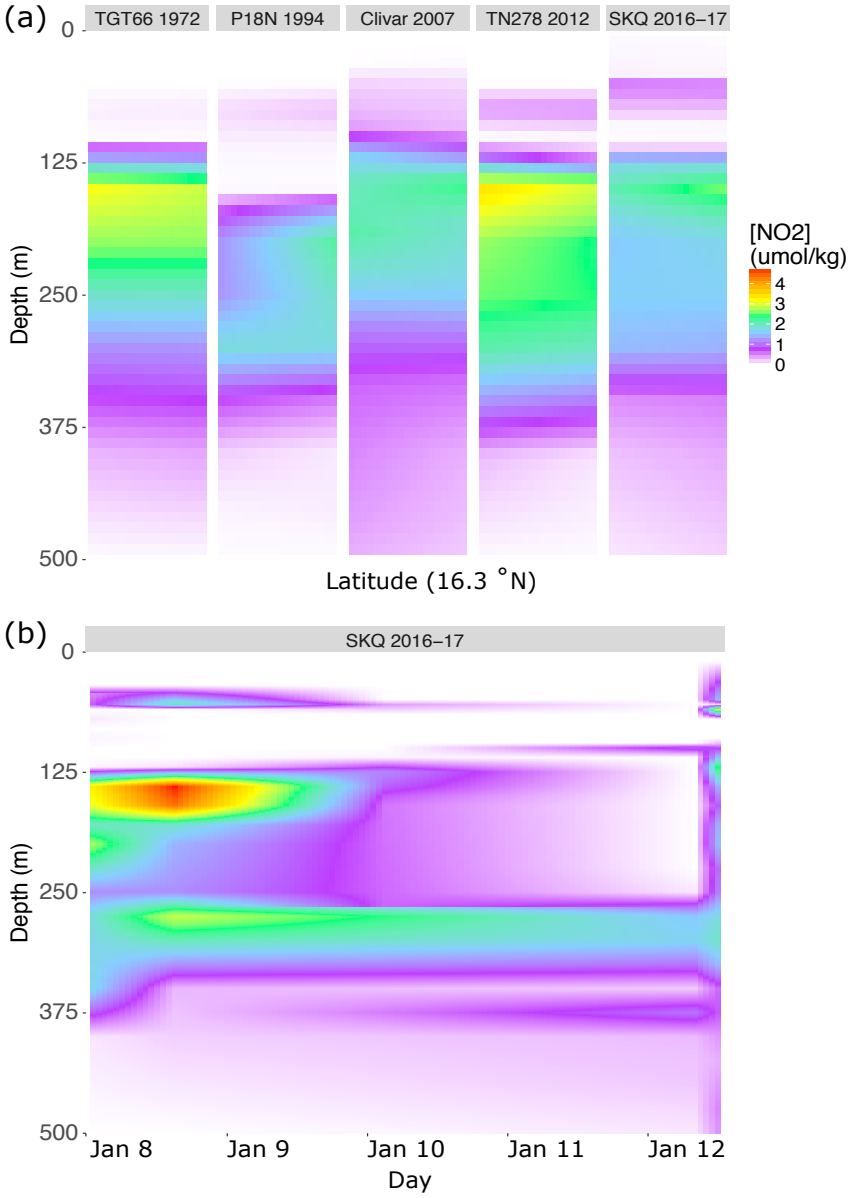

Figure 2 (a) Change in [NO_2^-] at 16.3˚ N for cruises TGT66 1972, P18N 1994, Clivar 2007, TN278 2012, and SKQ 2016-17 plotted by depth. NO_2^- values are from linear interpolations between CTD casts (see Figure 1). **(b)** [NO_2^-] measured over five continuous days from time-series Station P2. These concentrations were measured onboard the SKQ 2016-17 cruise using the azo dye method.

The vertical extent of the ODZ increased from the TGT001 1965 cruise to the SKQ 2016-17 cruise. A Wilcoxon signed rank test showed that the increase was significant, with a p-value < 0.0078 (Appendix B). The increase in vertical extent, or thickness, appears to be related to both time and ENSO state (Figure 3). The color shading of the boxes show ENSO state of the 4 months prior to the cruise, indicating that the first two cruises happened during a moderate El Niño and a weak El Niño, respectively, and the last few, excluding P18N, happened during weak La Niña. P18N was during neither condition. La Niña conditions appear to be associated with an increase in the ODZ vertical depth, although not significantly (p-value of 0.50).

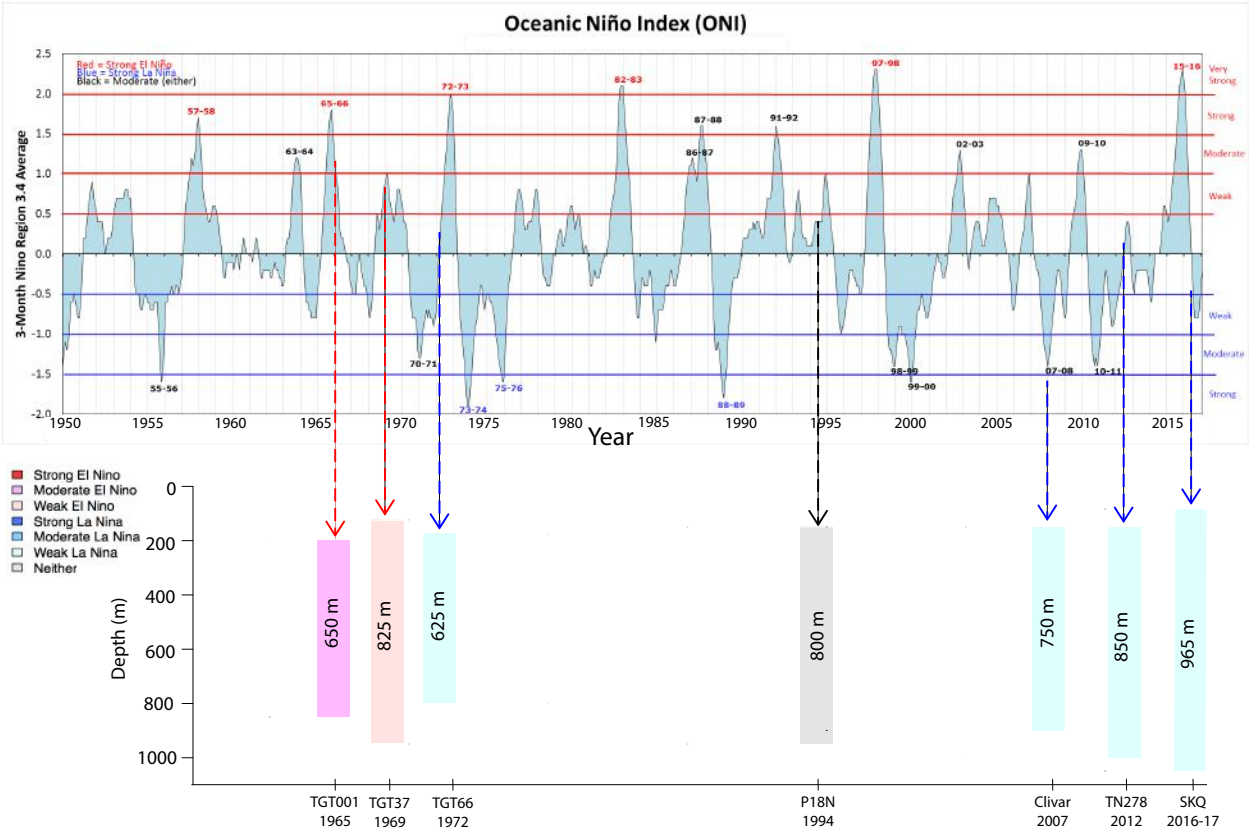

Figure 3 The ONI from NOAA represents ENSO intensities from neither to weak to strong (top). Snapshots of ODZ thickness in certain years are indicated with dashed arrows (blue during "La Niña cruises," red during "El Niño cruises"). The colors of the bars represent ENSO state during the cruise, calculated by the averaged ONI values from the 4 months leading up to the cruise. Both the depth at which the ODZ sits in the water column and ODZ thickness are graphically illustrated (bottom). Color bars are spaced respective to each ETNP cruise.

There is an overall upward trend of ODZ thickness, signifying expansion over time, and an overall downward trend of the ODZ top boundary over time, signifying shoaling of the top boundary (Figure 4). ODZ thickness and ONI have a correlation coefficient of -0.3086 (Figure 4a). Negative correlation between these two variables signifies that as the ODZ expands, ONI values decrease (La Niña conditions). La Niña and ODZ thickness were not statistically significantly correlated (Appendix B). The depth at which NO_2^- reached 0.3 µmol/kg and ONI values have a positive correlation, although the lack of data do not allow for any significant conclusions to be made (Figure 4b). The depth at which NO_2^- reached 0.3 µmol/kg and the depth at which NO_3^- reached 15 µmol/kg are positively correlated, showing that as NO_2^- maxima

deepen, the depth where NO_3^- concentrations drop up deepens as well (Figure 4c). This correlation was not statistically significant either. The top boundary of the ODZ and the depth at which NO_2^- reached 0.3 µmol/kg were positively correlated, signifying that as the ODZ deepens, the NO2 maxima deepen as well (Figure 4d). These correlations were not statistically significant. More correlation tests were done (Appendix B). Most of the correlation coefficients between two properties were not very high, the majority of them falling below r = 0.5. The only statistically significant correlation ($p < 0.05$) was ONI versus SiO_4^{2-}, though this apparent correlation may have emerged due to random chance from multiple comparisons. With a Bonferroni Correction (11 tests), there is a 43% chance of observing at least one statistically significant value.

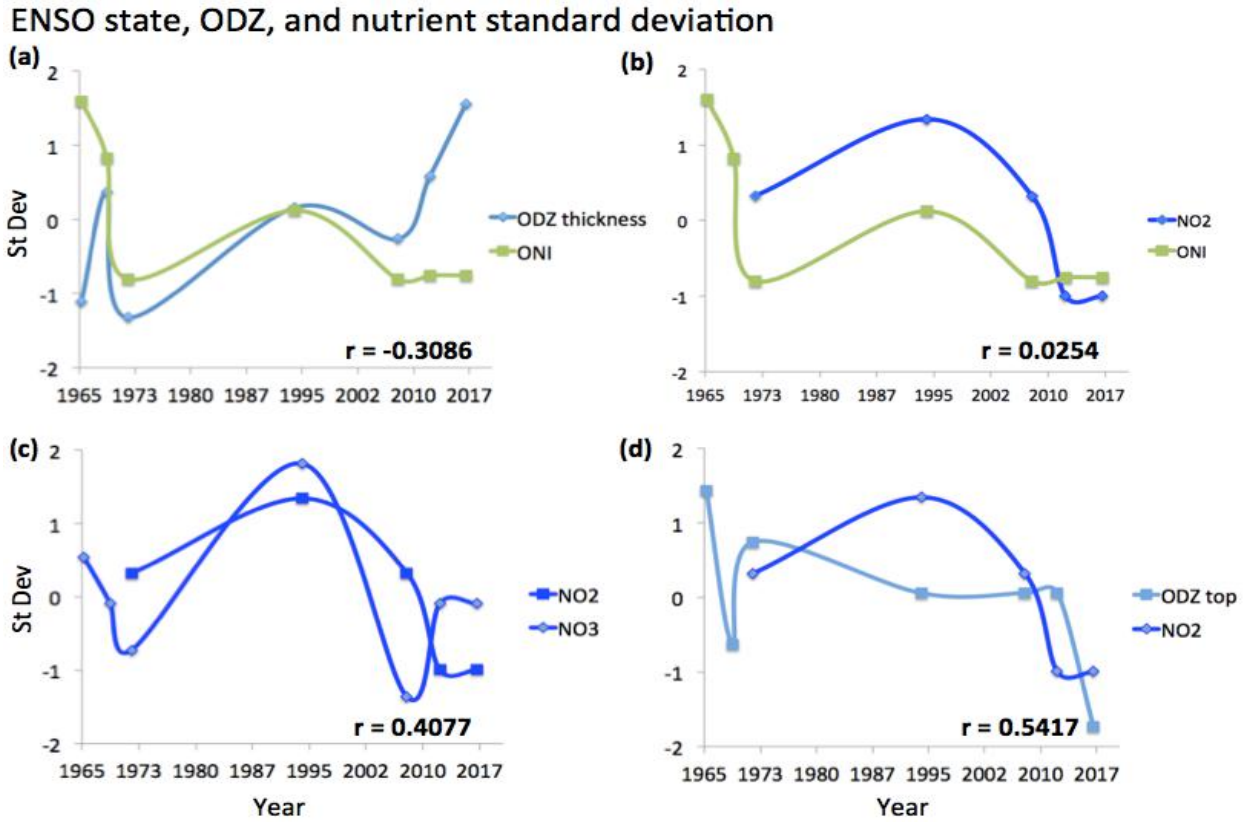

Figure 4 (a) ONI values (green) are negatively correlated with ODZ thickness (blue). (b) ONI values are positively correlated with NO_2^- (purple). (b) NO_2^- is positively correlated with NO_3^- (purple). (d) ODZ top boundary (blue) is correlated with NO_2^-. Correlation coefficient between properties is shown (r).

DISCUSSION

This study not only provides an additional set of data to an ongoing research effort to understand nutrient distribution in oxygen deficient waters off the coast of Mexico but also allows us to examine the correlations with ENSO state. The results from this study support the observations that suggest that the boundaries of the ODZ are expanding over time, and that nutrient distributions are following (Horak et al. 2016, Fiedler and Talley, 2006, Czeschel et al. 2012). Processes that drive oxygen deficiency include (1) high biological productivity and export, (2) influx of O_2 deficient water, (3) decreased influx of new O_2-rich water, and (4) increased global temperature. This study did not statistically significantly prove that either El Niño or La Niña

caused ODZ vertical expansion, though they both could be acting with one another to drive expansion. During La Niña, nutrients from deep water replenish the surface, first increasing primary production and then causing O_2 consumption through respiration (1). As opposed to upwelling from deep, oxygenated water, the source of the upwelled water could be the ODZ as seen by Nam et al. (2011), so the resulting upwelled water is deficient to begin with (2). During El Niño, strong thermoclines impede convection of colder, deeper water, which holds more O_2 (3). Increased global temperature has also been related to ODZ expansion, as seen in Stramma et al. (2010) (4). Since global temperature is tightly linked to ENSO state, ENSO conditions were examined relative to ODZ vertical expansion.

Figure 3 provides a compelling visualization showing how the ODZ and ENSO state are related to one another. Although five out of seven cruises occurred during were during weak conditions and one cruise during neither condition, with more continuous monitoring of the ODZ vertical extent, the gaps between cruise years could be filled. Continuous monitoring and sampling in the ETNP during strong conditions might provide strong enough evidence to prove that either El Niño or La Niña are driving an increase in ODZ thickness. An alternate hypothesis to be examined is that both are acting together as stated above. This would be a reasonable conclusion because low O_2 conditions are cumulative; each year represents the O_2 loss from the previous year and the year before that. O_2 concentrations are not replenished as easily since no aerobic organisms produce O_2 in the ODZ, and influx of O_2 from outside is the only source of O_2. In contrast, nutrient distributions, like NO_2^-, appear to be momentary snapshots in time.

Horak et al. (2016) concluded that deoxygenation and increased ODZ thickness caused more N_2 gas to be lost over time through denitrification. Although $[NO_2^-]$ was unusually high (3 μmol/kg to 4 μmol/kg) during the TN278 cruise, $[NO_2^-]$ rarely exceeded 4 μmol/kg during the SKQ 2016-17 cruise, even though the ODZ thickness was greater in 2016-17. Our observation that NO_2^- shows greater daily variability than yearly variability suggests that supposed inter-annual variability in $[NO_2^-]$ might instead be due to random sampling in an environment that varies on shorter time-scales. The conclusion that deoxygenation and N_2 loss by denitrification is increasing may have been based off of a coincidental high NO_2^- measurement during the TN278 cruise. Comparison of NO_2^- heat maps among years only represents a snapshot in time of the $[NO_2^-]$ on the day the seawater was collected. In other words, NO_2^- fluctuates daily, so comparison between years is inconclusive.

Instead, NO_2^- distribution and its in correlation to the ODZ top boundary is a more informative way to evaluate NO_2^-. The construction of the ODZ affects nutrient distributions, which then have an effect on the biology of the ecosystem, and ultimately on the N cycle. As seen previously, the NO_2^- maxima occur at the top of the ODZ, which is shoaling with time. As the ODZ shoals, the NO_2^- maxima shoal as well, causing fixed N in the surface ocean to be removed as N_2 gas.

Aerobic organisms cannot survive in ODZs both because of the lack of oxygen and because denitrifiers are removing nutrients they need for growth. Phytoplankton are one of the most important primary producers of the entire planet, producing half of the oxygen that enters the atmosphere (Nielsen, 1952). If phytoplankton production is altered, there could be drastic implications on both CO_2 uptake and O_2 release from the ETNP. Our study shows low to no

nutrients in the surface ocean, suggesting that biological processes are using them up. PO_4^{3-} and SiO_4^{2-} are nutrients needed by phytoplankton and diatoms, which occupy the surface of the ocean and cause surface [PO_4^{3-}] and [SiO_4^{2-}] to be low (Appendix Ab, Ac). Diatoms need SiO_4^{2-} to create frustules (Thomas and Dodson, 1974) and phytoplankton need PO_4^{3-} for growth (Geider and La Roche, 2002).

As climate change accelerates and ocean temperatures warm, the ocean will become more stratified and less capable of holding O_2 (Stramma et al., 2010). Climate models over geologic time show a decrease in dissolved O_2 concentrations paired with an expansion of OMZs (Matear et al., 2000; Oschlies, 2009). A decrease in O_2 concentrations has also been modeled to predict faster rates of denitrification - N removal - and nutrient limitation of primary production (Deutsch et al., 2011). Nutrient distribution and ODZ thickness in the ETNP have an important relationship with one another. The ODZ has increased over 300 m since 1965, and it is now almost 50% larger in vertical extent today. It has not only been deepening, but also shoaling; oxygen deficiency is impinging on the surface ocean where biological processes occur. Whether or not ENSO is driving this rapid increase in ODZ vertical extent, it crucial to understand how these oxygen deficient systems are changing and what that could imply for our oceans.

ACKNOWLEDGEMENTS

I want to extend my thanks to Rick Keil and his lab, including Jaqui Neibauer and Megan Duffy, who gave me the chance to conduct this research project in the ETNP. I also thank the crewmembers and scientists aboard the *R/V Sikuliaq* who contributed to my data collection and to Rachel Horak who shared her data with me. All of my analysis in R Studio would not have been as complete as it is without the help of Jacob Cram, who also spent the time to mentor me through my data analysis. And I want to thank Julian Sachs, Arthur Nowell, and LuAnne Thompson who have helped review my thesis and provide critical feedback. I am also grateful for my peers in the School of Oceanography, especially Jamee Adams and Marisa Borreggine, who have provided so much support and feedback throughout the year.

REFERENCES

Brunner, B., S. Contreras, M. F. Lehmann, O. Matantseva, M. Rollog, T. Kalvelage, G. Klockgether, G. Lavik, M. S. M. Jetten, B. Kartal, and M. M. M. Kuypers, 2013, Nitrogen isotope effects induced by anammox bacteria: Proceedings of the National Academy of Sciences of the United States of America, v. 110, p. 18994-18999.

Bullister, John L., and Gregory C. Johnson. "Cruise Report: P18_2007." (2008): n. pag. Web. 2 Dec. 2016.

Camargo, J. A., and A. Alonso, 2006, Ecological and toxicological effects of inorganic nitrogen pollution in aquatic ecosystems: A global assessment: Environment International, v. 32, p. 831-849.

Cane, M. A., 2005, The evolution of El Nino, past and future: Earth and Planetary Science Letters, v. 230, p. 227-240.

Codispoti, L. A., and F. A. Richards, 1976, Analysis Of Horizontal Regime Of Denitrification In Eastern Tropical North Pacific: Limnology and Oceanography, v. 21, p. 379-388.

Czeschel, R., L. Stramma, and G. C. Johnson, 2012, Oxygen decreases and variability in the eastern equatorial Pacific: Journal of Geophysical Research-Oceans, v. 117, p. 12.

Deutsch, C., H. Brix, T. Ito, H. Frenzel, and L. Thompson, 2011, Climate-Forced Variability of Ocean Hypoxia: Science, v. 333, p. 336-339.

Fiedler, P. C., and L. D. Talley, 2006, Hydrography of the eastern tropical Pacific: A review: Progress in Oceanography, v. 69, p. 143-180.

Geider, R. J., and J. La Roche, 2002, Redfield revisited: variability of C : N : P in marine microalgae and its biochemical basis: European Journal of Phycology, v. 37, p. 1-17.

Horak, R. E. A., W. Ruef, B. B. Ward, and A. H. Devol, 2016, Expansion of denitrification and anoxia in the eastern tropical North Pacific from 1972 to 2012: Geophysical Research Letters, v. 43, p. 5252-5260.

Karstensen, J., L. Stramma, and M. Visbeck, 2008, Oxygen minimum zones in the eastern tropical Atlantic and Pacific oceans: Progress in Oceanography, v. 77, p. 331-350.

Knap, A. H., Michaels, A. F., Dow, R. L., Johnson, R. J., Gundersen, K., Sorensen, J. C., Close, A. R., Howse, F., Hammer, M., Bates, N., Doyle, A., Waterhouse, T., 1993a. BATS Methods Manual, Version 3. U.S. JGOFS Planning O$ce, Woods Hole, MA.

Liu, X. D., S. M. Tiquia, G. Holguin, L. Y. Wu, S. C. Nold, A. H. Devol, K. Luo, A. V. Palumbo, J. M. Tiedje, and J. Z. Zhou, 2003, Molecular diversity of denitrifying genes in continental margin sediments within the oxygen-deficient zone off the Pacific coast of Mexico: Applied and Environmental Microbiology, v. 69, p. 3549-3560.

Matear, R. J., A. C. Hirst, and B. I. McNeil, 2000, Changes in dissolved oxygen in the Southern Ocean with climate change: Geochemistry Geophysics Geosystems, v. 1.

Nam, S., H. J. Kim, and U. Send, 2011, Amplification of hypoxic and acidic events by La Nina conditions on the continental shelf off California: Geophysical Research Letters, v. 38, p. 5.

Nielsen, E. Steemann. "The use of radio-active carbon (C14) for measuring organic production in the sea." Journal du Conseil 18.2 (1952): 117-140.

Oschlies, A., 2009, Simulated 21(st) century's increase in oceanic suboxia by CO2-enhanced biotic carbon export: Geochimica Et Cosmochimica Acta, v. 73, p. A977-A977.

Penn, J., T. Weber, and C. Deutsch, 2016, Microbial functional diversity alters the structure and sensitivity of oxygen deficient zones: Geophysical Research Letters, v. 43, p. 9773-9780.

Sarmiento, Jorge L., Timothy D. Herbert, and J. R. Toggweiler. "Causes of Anoxia in the World

Ocean." Global Biogeochemical Cycles 2.2 (1988): 115-28. Web.
Stramma, L., S. Schmidtko, L. A. Levin, and G. C. Johnson, 2010, Ocean oxygen minima expansions and their biological impacts: Deep-Sea Research Part I-Oceanographic Research Papers, v. 57, p. 587-595.
Strickland, J.D.H. and Parsons, T.R. 1972 A practical handbook of seawater analysis. 2nd edition. Bull. Fish. Res. Bd Canada, **167**, 310 pp.
Taft, Bruce, and Gregory Johnson. "WHP Cruise Summary Information." (1994): n. pag. Web. 2 Dec. 2016.
Thomas, W. H., and A. N. Dodson, 1974, Inhibition Of Diatom Photosynthesis By Germanic Acid - Separation Of Diatom Productivity From Total Marine Primary Productivity: Marine Biology, v. 27, p. 11-19.
Tsementzi, D., J. Y. Wu, S. Deutsch, S. Nath, L. M. Rodriguez, A. S. Burns, P. Ranjan, N. Sarode, R. R. Malmstrom, C. C. Padilla, B. K. Stone, L. A. Bristow, M. Larsen, J. B. Glass, B. Thamdrup, T. Woyke, K. T. Konstantinidis, and F. J. Stewart, 2016, SAR11 bacteria linked to ocean anoxia and nitrogen loss: Nature, v. 536, p. 179-+.

APPENDIX

Appendix A

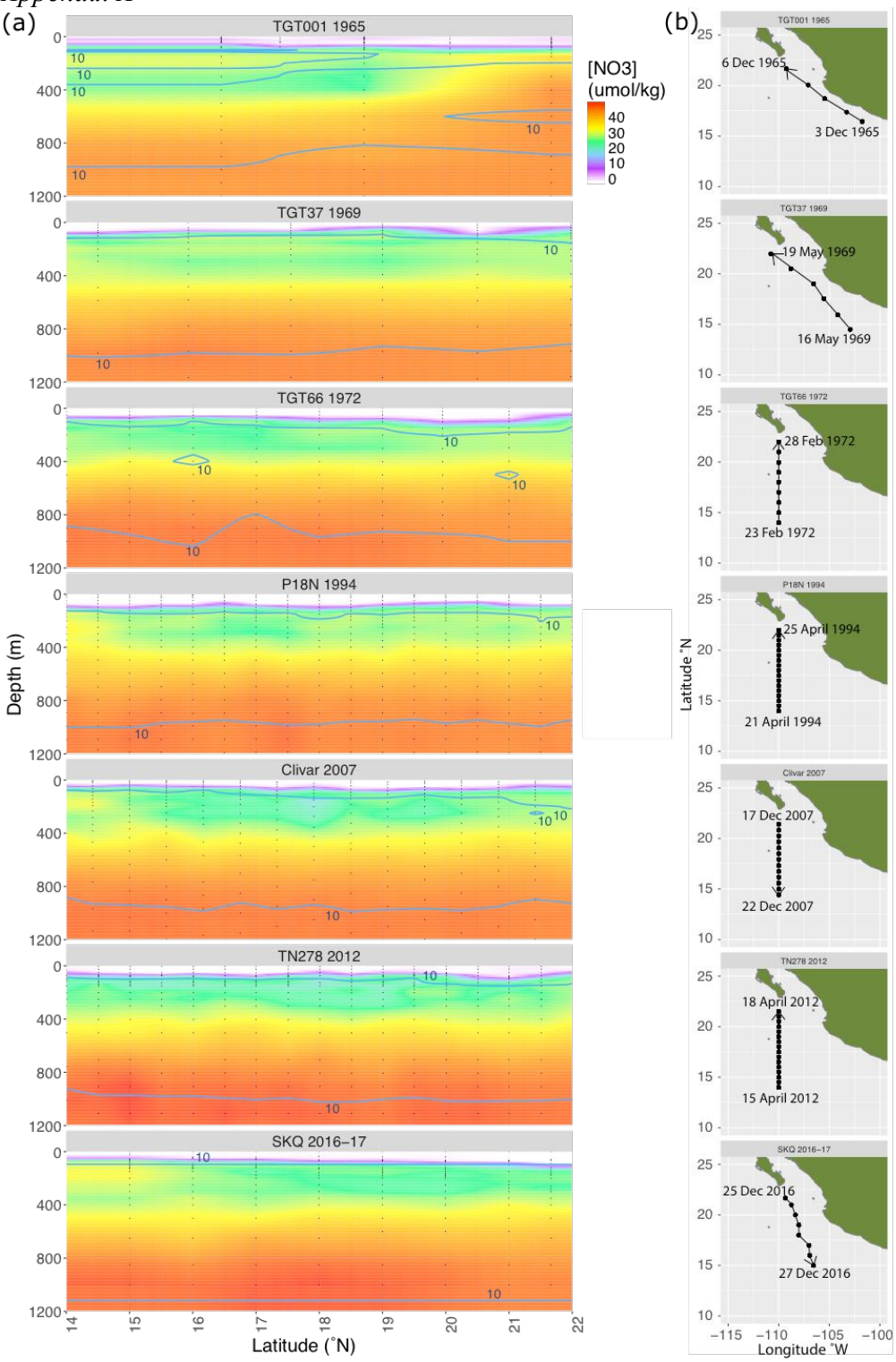

Appendix Aa (a) [NO_3^-] as a heat map from 14˚ N to 22.5˚ N. All seven cruises (TGT001, TGT37, TGT66, P18N, Clivar, TN278, SKQ) collected NO_3^- data. Vertical dots show where seawater was collected and [NO_3^-] was measured. Spaces between CTD casts are linearly interpolated by depth and latitude. Oxygen contour lines are plotted at 10 µmol/kg. **(b)** Cruise transects off the coast of Baja California and Mexico.

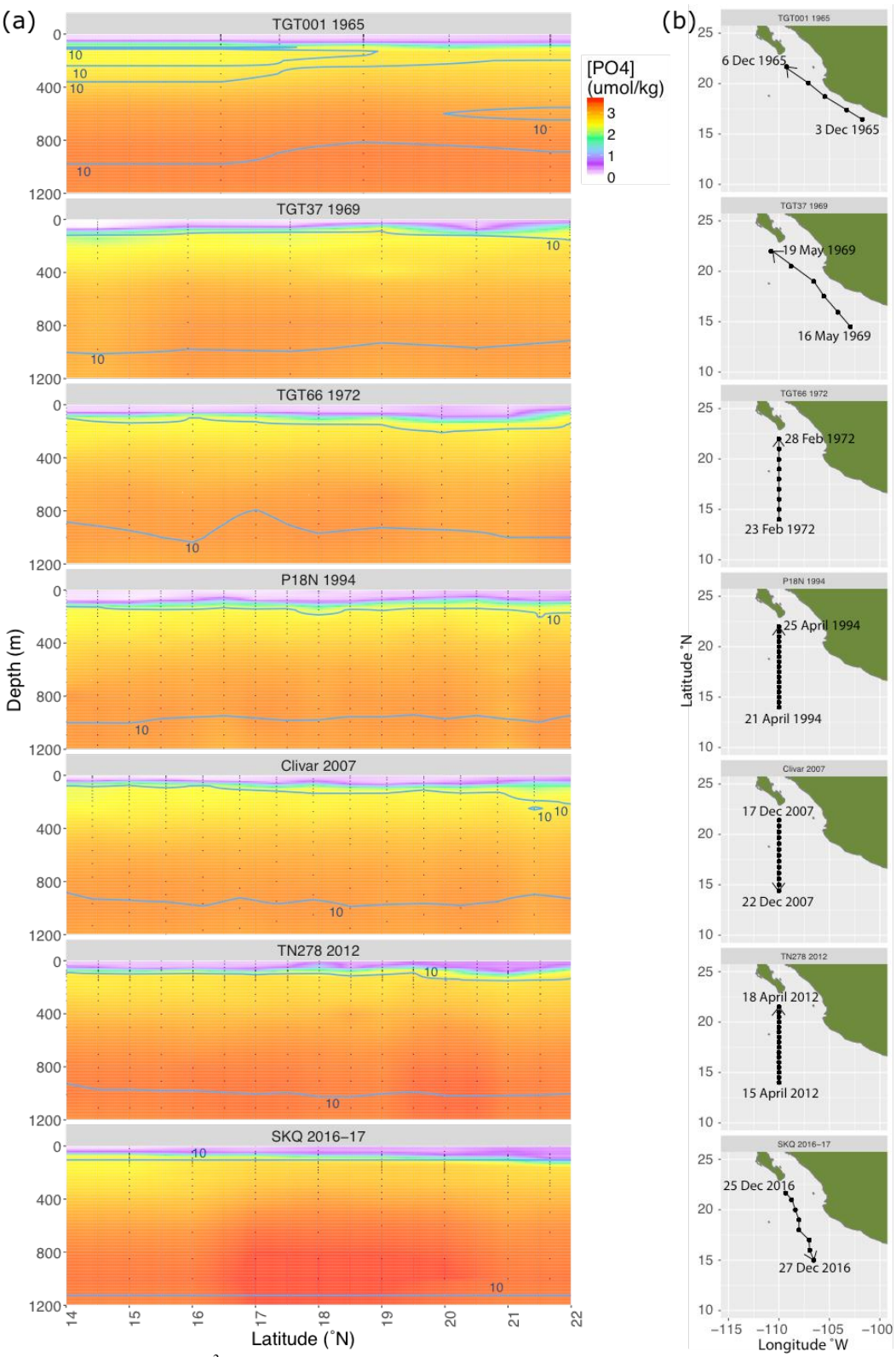

Appendix Ab (a) [PO_4^{3-}] as a heat map from 14˚ N to 22.5˚ N. All seven cruises (TGT001, TGT37, TGT66, P18N, Clivar, TN278, SKQ) collected PO_4^{3-} data. Vertical dots show where seawater was collected and [PO_4^{3-}] was measured. Spaces between CTD casts are linearly interpolated by depth and latitude. Oxygen contour lines are plotted at 10 µmol/kg. **(b)** Cruise transects off the coast of Baja California and Mexico.

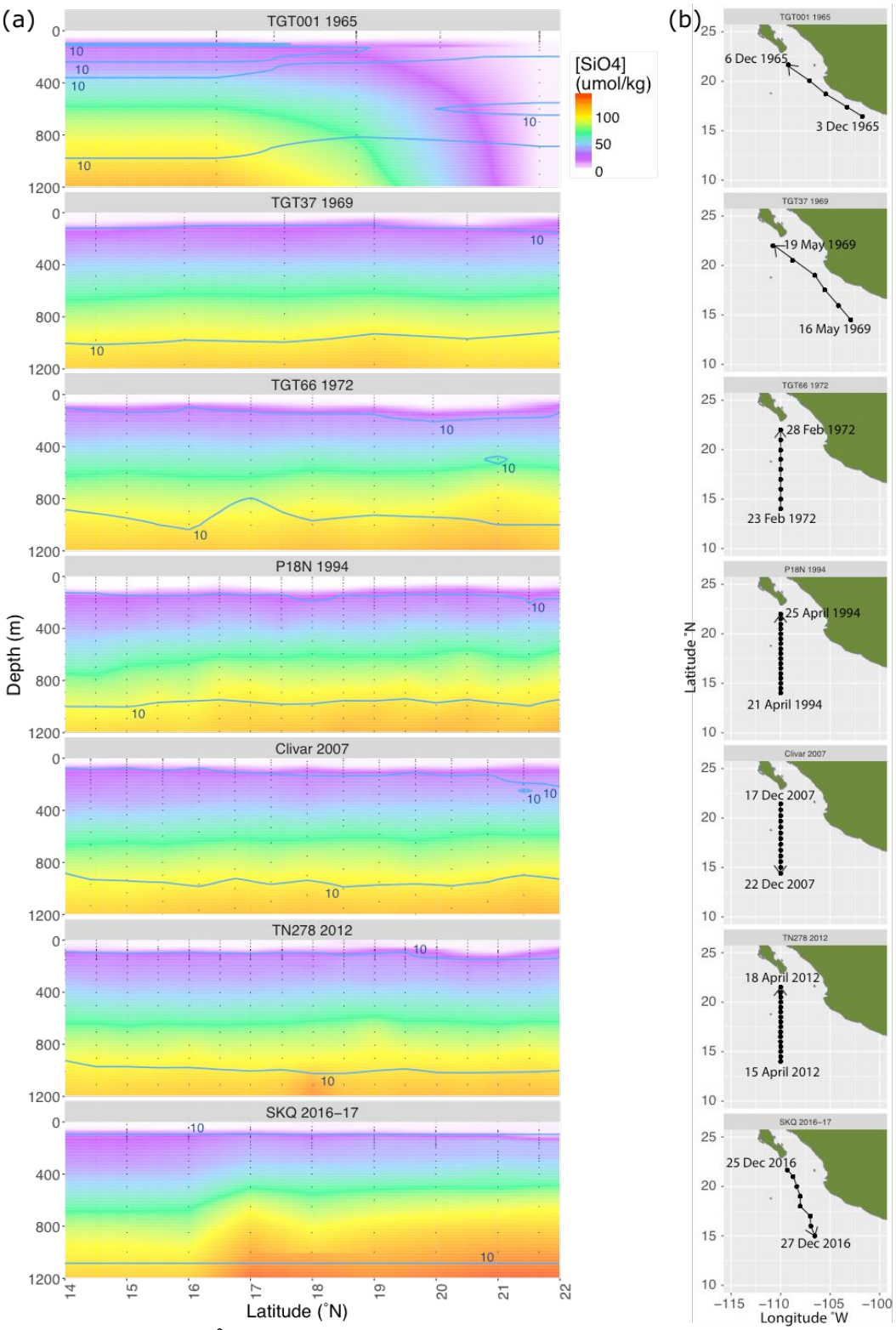

Appendix Ac (a) [SiO_4^{2-}] as a heat map from 14˚ N to 22.5˚ N. All seven cruises (TGT001, TGT37, TGT66, P18N, Clivar, TN278, SKQ) collected SiO_4^{2-} data. Vertical dots show where seawater was collected and [SiO_4^{2-}] was measured. Spaces between CTD casts are linearly interpolated by depth and latitude. Oxygen contour lines are plotted at 10 µmol/kg. **(b)** Cruise transects off the coast of Baja California and Mexico.

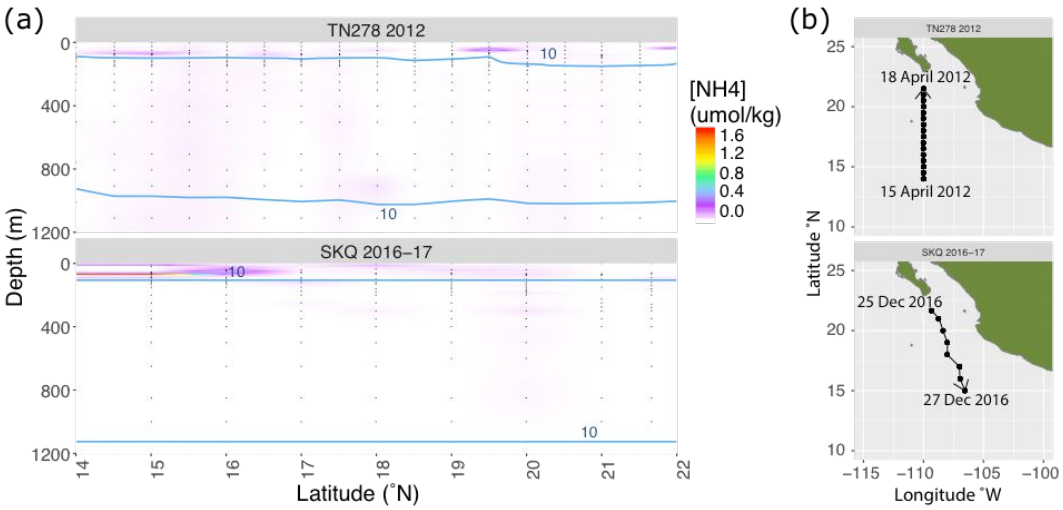

Appendix Ad (a) [NH_4^+] as a heat map from 14˚ N to 22.5˚ N. Only two cruises (TN278, SKQ) collected NH_4^+ data. Vertical dots show where seawater was collected and [NH_4^+] was measured. Spaces between CTD casts are linearly interpolated by depth and latitude. Oxygen contour lines are plotted at 10 µmol/kg. **(b)** Cruise transects off the coast of Baja California and Mexico.

Appendix B

Standard Deviation Correlation Statistics

Properties	Slope	Intercept	Corr. Coeff. (r)	n	R^2	t-value	p-value
ONI ~ ODZ vert	-0.30	-0.08	-0.31	7	0.10	-0.73	0.50
ONI ~ ODZ top	1.29	6.85	0.41	7	0.17	1.01	0.36
ONI ~ NO2	0.02	-0.14	0.03	5	0.00	0.04	0.97
ONI ~ NO3	0.47	-0.08	0.49	7	0.24	1.25	0.27
ONI ~ PO4	0.15	-0.08	0.15	7	0.02	0.34	0.75
ONI ~ SiO4	0.80	-0.08	0.83	7	0.68	3.28	0.02
ODZ top ~ NO2	0.50	-0.16	0.54	5	0.29	1.12	0.35
ODZ top ~ NO3	0.08	0.00	0.08	7	0.01	0.18	0.87
ODZ top ~ PO4	0.15	0.00	0.15	7	0.02	0.35	0.74
ODZ top ~ SiO4	0.67	0.00	0.67	7	0.45	2.04	0.10
NO2 ~ NO3	0.48	-0.09	0.41	5	0.17	0.77	0.50

Wilcoxon Test p-value: 0.007813

Appendix B Statistical analysis on correlations between ENSO, ODZ, and nutrient distributions.

Appendix C

Running 3-Month Mean ONI Values

Year	DJF	JFM	FMA	MAM	AMJ	MJJ	JJA	JAS	ASO	SON	OND	NDJ
1962	-0.2	-0.2	-0.2	-0.3	-0.3	-0.2	-0.1	-0.2	-0.2	-0.3	-0.3	-0.4
1963	-0.4	-0.2	0.1	0.2	0.2	0.4	0.7	1.0	1.1	1.2	1.2	1.1
1964	1.0	0.6	0.1	-0.3	-0.6	-0.6	-0.7	-0.7	-0.8	-0.8	-0.8	-0.8
1965	-0.5	-0.3	-0.1	0.1	0.4	0.7	1.0	1.3	1.6	1.7	1.8	1.5
1966	1.3	1.0	0.9	0.6	0.3	0.2	0.2	0.1	0	-0.1	-0.1	-0.3
1967	-0.4	-0.5	-0.5	-0.5	-0.2	0	0	-0.2	-0.3	-0.4	-0.4	-0.5
1968	-0.7	-0.8	-0.7	-0.5	-0.1	0.2	0.5	0.4	0.3	0.4	0.6	0.8
1969	0.9	1.0	0.9	0.7	0.6	0.5	0.4	0.5	0.8	0.8	0.8	0.7
1970	0.6	0.4	0.4	0.3	0.1	-0.3	-0.6	-0.8	-0.8	-0.8	-0.9	-1.2
1971	-1.3	-1.3	-1.1	-0.9	-0.8	-0.7	-0.8	-0.7	-0.8	-0.8	-0.9	-0.8
1972	-0.7	-0.4	0	0.3	0.6	0.8	1.1	1.3	1.5	1.8	2.0	1.9
1973	1.7	1.2	0.6	0	-0.4	-0.8	-1.0	-1.2	-1.4	-1.7	-1.9	-1.9
1974	-1.7	-1.5	-1.2	-1.0	-0.9	-0.8	-0.6	-0.4	-0.4	-0.6	-0.7	-0.6
1975	-0.5	-0.5	-0.6	-0.6	-0.7	-0.8	-1.0	-1.1	-1.3	-1.4	-1.5	-1.6
1990	0.1	0.2	0.2	0.2	0.2	0.3	0.3	0.3	0.4	0.3	0.4	0.4
1991	0.4	0.3	0.2	0.2	0.4	0.6	0.7	0.7	0.7	0.8	1.2	1.4
1992	1.6	1.5	1.4	1.2	1.0	0.8	0.5	0.2	0	-0.1	-0.1	0
1993	0.2	0.3	0.5	0.7	0.8	0.6	0.3	0.2	0.2	0.2	0.1	0.1
1994	0.1	0.1	0.2	0.3	0.4	0.4	0.4	0.4	0.4	0.6	0.9	1.0
1995	0.9	0.7	0.5	0.3	0.2	0	-0.2	-0.5	-0.7	-0.9	-1.0	-0.9
1996	-0.9	-0.7	-0.6	-0.4	-0.2	-0.2	-0.2	-0.3	-0.3	-0.4	-0.4	-0.5
1997	-0.5	-0.4	-0.2	0.1	0.6	1.0	1.4	1.7	2.0	2.2	2.3	2.3
2003	0.9	0.7	0.4	0	-0.2	-0.1	0.1	0.2	0.2	0.3	0.3	0.3
2004	0.3	0.3	0.2	0.1	0.2	0.3	0.5	0.6	0.7	0.7	0.6	0.7
2005	0.7	0.6	0.5	0.5	0.3	0.2	0	-0.1	0	-0.2	-0.5	-0.7
2006	-0.7	-0.6	-0.4	-0.2	0.0	0.0	0.1	0.3	0.5	0.7	0.9	0.9
2007	0.7	0.4	0.1	-0.1	-0.2	-0.3	-0.4	-0.6	-0.9	-1.1	-1.3	-1.3
2008	-1.4	-1.3	-1.1	-0.9	-0.7	-0.5	-0.4	-0.3	-0.3	-0.4	-0.6	-0.7
2009	-0.7	-0.6	-0.4	-0.1	0.2	0.4	0.5	0.5	0.6	0.9	1.1	1.3
2010	1.3	1.2	0.9	0.5	0.0	-0.4	-0.9	-1.2	-1.4	-1.5	-1.4	-1.4
2011	-1.3	-1.0	-0.7	-0.5	-0.4	-0.3	-0.3	-0.6	-0.8	-0.9	-1.0	-0.9
2012	-0.7	-0.5	-0.4	-0.4	-0.3	-0.1	0.1	0.3	0.3	0.3	0.1	-0.2
2013	-0.4	-0.4	-0.3	-0.2	-0.2	-0.2	-0.3	-0.3	-0.2	-0.3	-0.3	-0.3
2014	-0.5	-0.5	-0.4	-0.2	-0.1	0.0	-0.1	0.0	0.1	0.4	0.5	0.6
2015	0.6	0.5	0.6	0.7	0.8	1.0	1.2	1.4	1.7	2.0	2.2	2.3
2016	2.2	2.0	1.6	1.1	0.6	0.1	-0.3	-0.6	-0.8	-0.8	-0.8	-0.7
2017	-0.4	-0.1	0.1									

Month(s) of cruise

4 months pre-cruise

Break in years

J = Jan, Jun, Jul

F = Feb

M = Mar, May

A = Apr, Aug

S = Sept

O = Oct,

N = Nov

D = Dec

Appendix C ONI values from NOAA. Numbers signify st devs away from a 50-year sea surface temperature mean in the Niño-3.4 region. La Niña conditions are in blue, El Niño conditions are in red, and neither condition is in black. Each number is a 3-month mean of ONI values. For this study, the highlighted numbers (yellow) were averaged to find conditions during the month(s) of each respective cruise (magenta box).

Appendix D

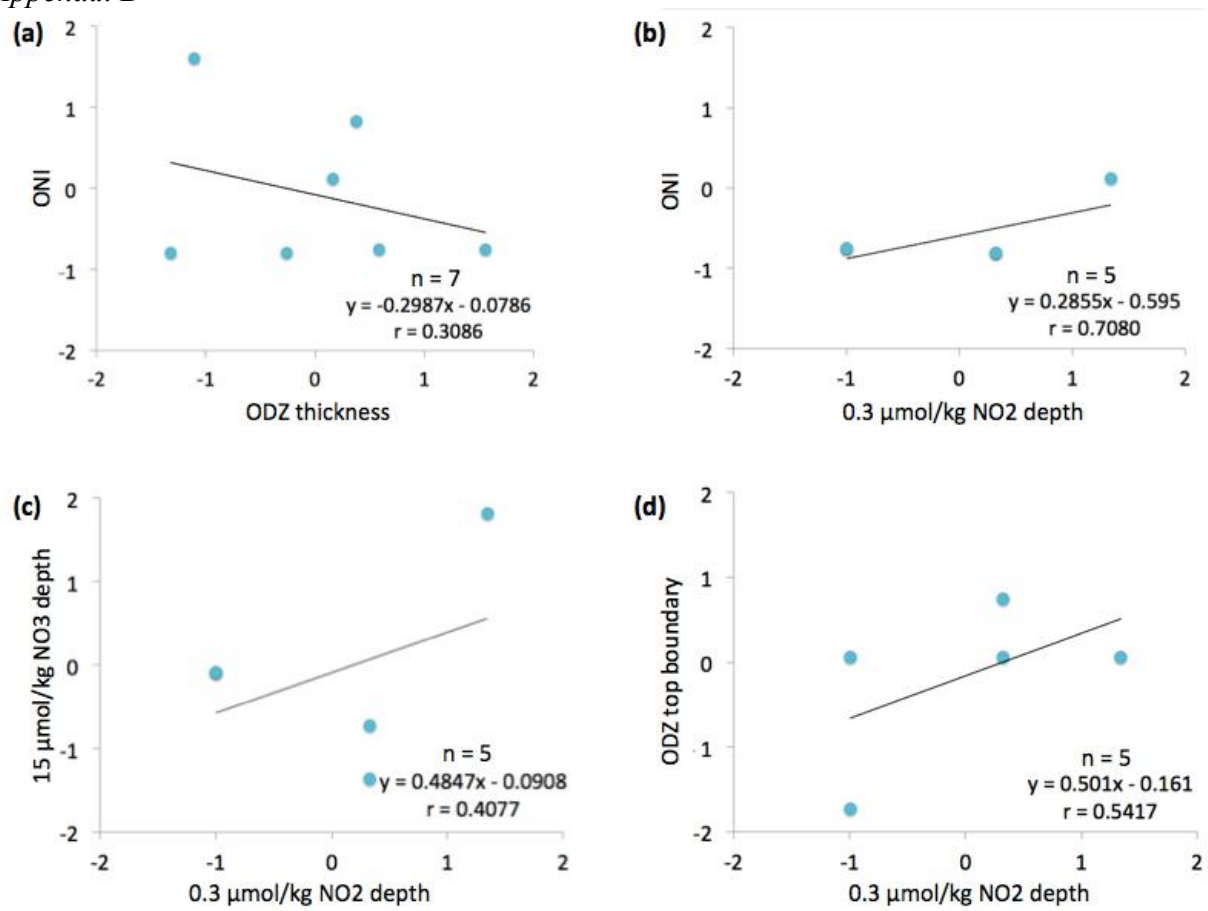

Appendix D These property-property plots are an extension of Figure 4. N is the number of samples (b, c, and d only had 5 samples because NO_2^- was not measured on TGT001 1965 and TGT37 1969). Refer to Figure 4 caption to understand how values were calculated. There is a negative relationship between ODZ thickness and ONI (a). There is a positive relationship between NO_2^- and ONI, NO_2^- and NO_3^-, and NO_2^- and the top boundary of the ODZ.